AN ULTRASENSITIVE VIBRATING PROBE FOR MEASURING STEADY EXTRACELLULAR CURRENTS

LIONEL F. JAFFE and RICHARD NUCCITELLI

From the Department of Biology, Purdue University, Lafayette, Indiana 47907

ABSTRACT

We describe a vibrating probe system for measuring relatively steady electrical current densities near individual living cells. It has a signal-to-noise ratio at least 100 times greater than previously available techniques. Thus it can be used to detect current densities as small as 10 nA/cm² in serum when a 30-μm diameter probe is vibrated at 200 Hz between two points 30 μm apart, and the amplifier's time constant is set at 10 s. Moreover, it should be generally insensitive to interference by concentration gradients. It has been first used to reveal and study 100-s long current pulses which developing fucoid embryos drive through themselves.

Present techniques seriously and unnecessarily limit measurement of the relatively steady electrical currents which living cells drive through themselves. By relatively steady currents, we mean currents that show little change in the course of seconds to hours. Such currents seem to be associated mainly with processes of cell growth, development, and transport, and may feed back to further polarize and differentiate cells (1). These currents may be contrasted with the better-studied ones which are mainly associated with neural communication and which change in the order of milliseconds.

Steady transcellular currents should generate steady intracellular voltage gradients, and in a few favorable cases, reproducible and relatively steady voltage differences have been measured intracellularly, i.e. between two probes inserted into two regions of the cytoplasm of the same cell (2), or into two cells connected by a cytoplasmic bridge (3). It remains uncertain, however, as to how much of each of these voltage differences really arose from an endogenous current, how much arose from an injury current produced by probe entry, and how much stemmed from a difference in fixed-charge density in the two regions. Moreover, intracellular voltage measurements are an insensitive as well as an ambiguous indicator of transcellular currents. Because of variations in so-called tip potentials, intracellular probes cannot be used reliably to detect differences smaller than about a millivolt; so in a typical case of two regions 30 μm apart in a cytoplasm with a resistivity of 300 Ω-cm, current densities smaller than about 1 mA/cm² would not be detected by this method.

Relatively steady transcellular currents might also be measured extracellularly. The use of extracellular probes can reduce or eliminate the problems of injury currents and of fixed-charge potentials; but it is only with a few favorable cells that it has yet proved possible to interrupt the extracellular current paths with resistances high enough to yield voltages measurable by conventional means. Using such *extracellular insulation*, Lund (4) measured voltage differences of the order of 1–30 mV outside of 4–8-mm long filaments of a freshwater alga; Tasaki and Kamiya (5) measured such differences outside of 200-μm long freshwater amebae, while Novák and Bentrup (6) did so outside of the 5-cm long unicellular marine alga,

Acetabularia. If supplemented with appropriate resistance data, such extracellular voltages might well yield useful measurements of the currents which traverse these cells. Moreover, Hagins et al. (7) measured voltage differences of the order of 10–100 μV along and between the closely packed 100-μm long photoreceptor cells of the rat retina, and did indeed convert these data into current values with the aid of appropriate resistance measurements. However, such extracellular insulation does not seem practical for most cells, e.g. for egg cells which are often spherical, isolated cells about 100 μm in diameter, coated with a 0.1-μm thick highly permeable gel, and growing in media containing at least 0.1 M salt. New methods are needed.

So some time ago, one of us obtained a measure of the current traversing developing fucoid eggs by a new *series method* (8). Several hundred eggs were lined up within a long, loose-fitting, seawater-filled capillary, and then polarized towards one end of the tube with unilateral light. This arrangement put the small (~0.3 μV) transcellular voltage differences in series, thus generating a voltage across the whole tube of the order of 100 μV. This was measured through some refinement of conventional means and converted to a rough but reliable transcellular current estimate. While reliable, this series method gave minimal spatial resolution and poor temporal resolution (since the development of the egg population is imperfectly synchronized), and depended upon a narrowly applicable method (photopolarization) of orienting this population. In this paper, we present a more exact and general solution to the problem of measuring steady transcellular currents.

MATERIALS AND METHODS

The Principle

The vibrating probe is used to measure the very minute fields near cells growing in a physiological medium. No effort is made to raise the external resistance; instead, probe noise is reduced enough to measure the tiny fields generated by transcellular currents while traversing even an unbounded and highly conductive medium. In fact the probe directly measures the voltage difference between the two extreme points of its vibration which are typically 30 μm apart. Since the electric field will be nearly constant over this small distance, it is approximately given by the voltage difference divided by this distance. The current density in the direction of the vibration and at the center of vibration is then given by this field multiplied by the medium's conductivity. The pattern given by a group of such measurements is then extrapolated to the cell's surface to give the size and pattern of the transcellular current.

The theoretical minimum noise introduced by a probe is the Johnson noise developed by its access resistance, i.e. by the resistance to current converging on the probe through the medium. Hitherto available probes are far noisier than this theoretical minimum for two fundamental reasons: first, because of their high resistance; and second, because of their high sensitivity to changes or gradients in the composition of the medium.

We have overcome these limitations and have approached the theoretical noise minimum by developing a method introduced by Davies (9). The idea is to vibrate a platinum-black electrode between two points in the cell's field. This converts any steady potential difference between these points into a sinusoidal AC output whose amplitude equals the potential difference and is measured with the aid of a lock-in amplifier. The volume resistance of the metallic electrode is of course negligible and *the impedance (hence Johnson noise) of the platinum-saline interface, being essentially capacitative, can be reduced to negligible values by sufficiently raising the vibration frequency* (10). Vibration likewise minimizes the effects both of uniform changes and of gradients in the composition of the medium. Uniform changes in composition should have a negligible effect because the same probe will experience practically the same changes in its two extreme positions. Gradients in composition will be reduced by the mixing action of the vibrating probe.

Description

The probe is shaped like a ballpoint pen, and is 11 mm long. The test electrode is a 20–30-μm diameter platinum-black coated *ball* at the probe's tip (part 20, Fig. 1); the reference electrode is a gross, platinum-black coated ring 0.6 mm behind this tip (part 19, Fig. 1). The probe is vibrated *laterally* so as to move its sensitive tip between two points in a cell's field (Fig. 2). (The two points are typically 30 μm apart.) This vibration also moves the reference electrode, but it is too far from the small sources studied to experience any voltage change. Thus the vibration converts any steady potential difference between the two points being compared into a sinusoidal probe output with a peak-to-peak amplitude equal to that steady difference.

This AC signal is amplified with the aid of a lock-in amplifier, and the probe is vibrated by a piezoelectric bender element driven by the amplified reference signal coming from this same lock-in amplifier (See Fig. 3 for a block diagram). This arrangement assures a constant phase relation between the probe's vibration and the oscillation of the signal-processing switches. The vibrated mass is reduced to about 0.5 g to raise the resonant frequency to about 200 Hz. This frequency is high enough to reduce the impedance at the metal-saline

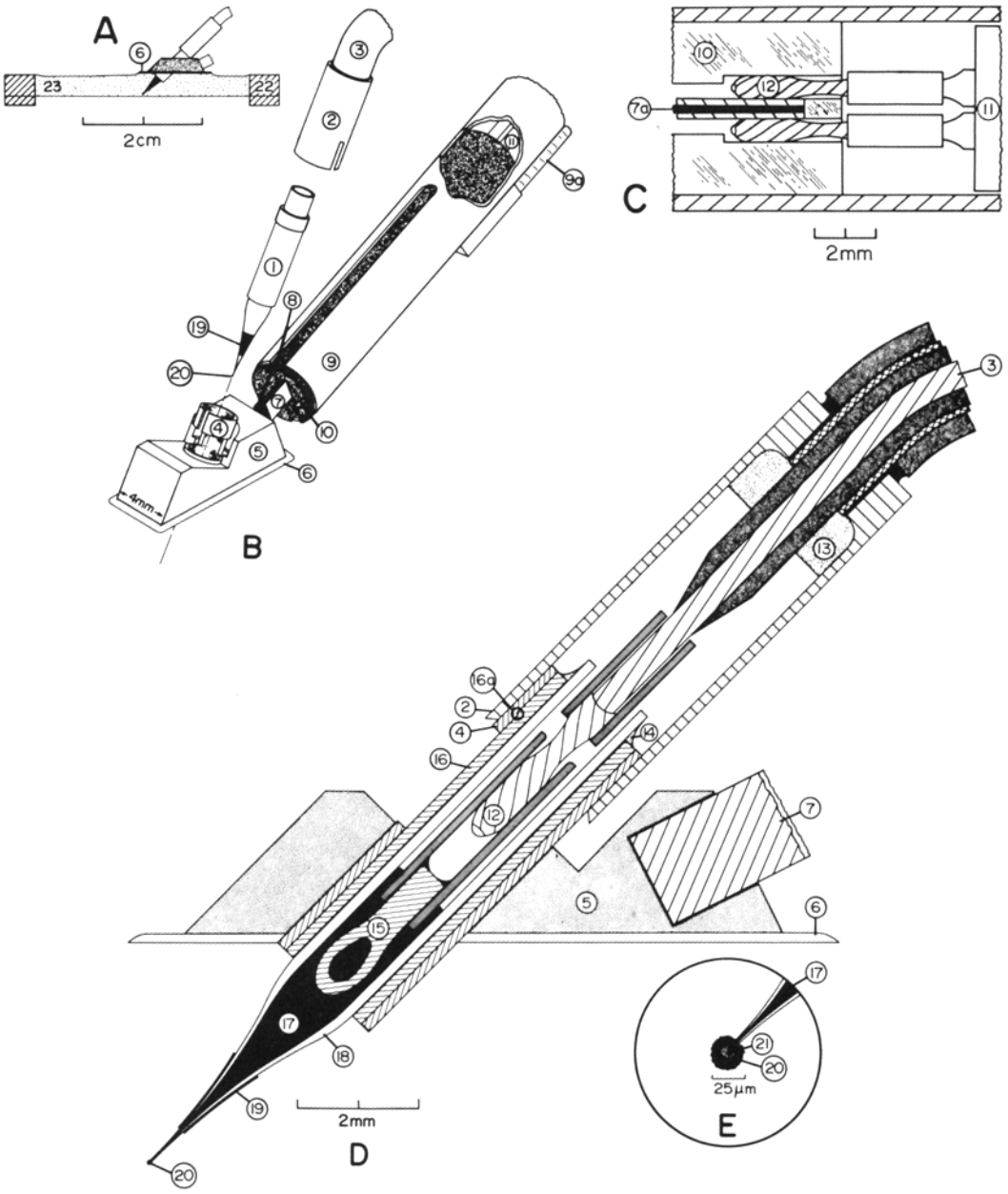

FIGURE 1 Vibrating probe. A. Near-natural size view of probe in measuring position. B. Exploded view of probe and vibrator. C. Detail of reed support. D. Detail of probe in holder. E. Detail of test electrode. Parts 1, Probe; 2, gold-plated brass cable connector; 3, signal cable (Gulton's Glennite C5HT); 4, gold-plated brass probe holders; 5, lucite block (cut-outs to minimize mass not shown); 6, inner boundary setter; 7, vibrating reed (Clevite's PZT5H bimorph bender, 0.54 × 1.6 × 22 mm); 7 *a*, brass center strip; 8, 0.2 mm grounded gold wire; 9, 6-gauge stainless steel tube; 9 *a*, dry air inlet tube (air enters at base of reed); 10, Kel-F support cylinder (distal end is gold plated); 11, bender power cable; 12, twist/con no. 24 pin (in the probe, this pin fits into a matching socket; at the vibrator's base, two such pins fit into no. 74 drill holes); 13 and 14, silicone rubber insulation; 15, no. 9 sewing needle eye; 16, gold-plated brass probe sleeve; 16 *a*, 3-mil step to stop probe from sliding through its holder; 17, Cerrotru solder; 18, glass pipette (drawn from 0.86-mm ID × 1.31 mm OD Pyrex stock); 19, platinum-black reference electrode; 20, platinum-black test electrode or ball; 21, gold seal; 22, specimen chamber (its bottom is cut from a no. 1 glass cover slip. This bottom is cemented between two lucite rings with silicone rubber aquarium cement to make a chamber); 23, culture medium, e.g. seawater.

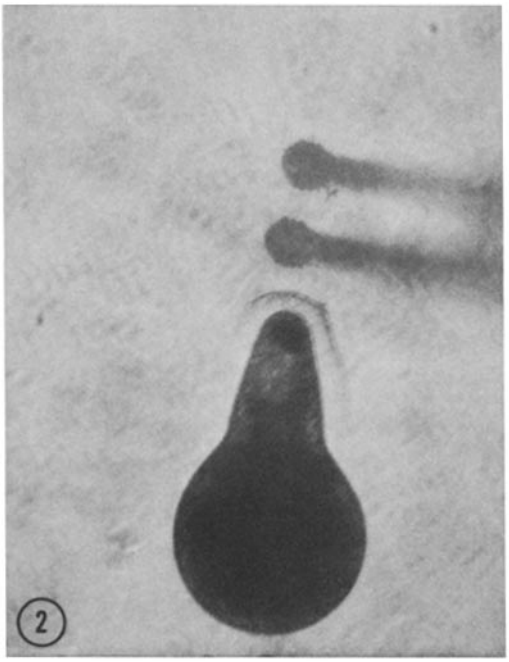

FIGURE 2 Photograph of a probe vibrating at 200 Hz in front of a growing, 1-day old *Pelvetia* embryo. Photographed under illumination by a stroboscope flashing at 400 Hz to visualize the probe in its two extreme positions. It is clearly visible in these positions even when steady illumination is used, but the contrast is improved by stroboscopic lighting. The sticky cell wall in front of the growing tip is outlined by adhering dirt. The embryo's smaller diameter is 100 μm.

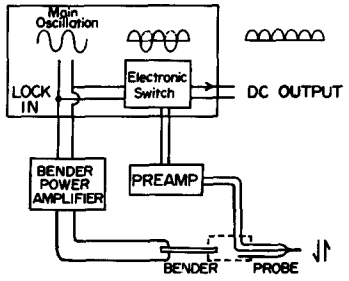

FIGURE 3 Vibrating probe system. The heart of the system is a Princeton Applied Research model 122 lock-in amplifier (Princeton Applied Research Corp., Princeton, N. J.). Its main oscillation is split into two parts. One part, tapped off the so-called reference port, is led to a bender power amplifier (consisting of an Analog Devices model 170 op amp (Analog Devices, Inc., Norwood, Mass.) and a resistance network). Thus amplified, it drives the bender which vibrates the probe. The probe's output goes to a P.A.R. model 112 preamp, then back into the lock-in. Within the lock-in an electronic switch, driven by the other part of the main oscillation, inverts alternating half-cycles of the signal to give an amplified DC output which goes to a Sargent model SRG chart recorder (Sargent-Welch Co., Skokie, Ill.).

interface from the extremely high, indeed ill-defined values found with direct current, down to about 10 kΩ. This low impedance in turn reduces the interfacial noise to an almost negligible level.

The bender is driven by about 10 V, while the probe, which is only 1 cm away, is sensitive to nanovolts. So it should not be surprising that leakage of current from the bender to the probe introduced serious artifacts in earlier models. These currents are reduced enough to eliminate such artifacts as follows: (*a*) the conductive silver coatings on the surfaces of the bender are removed from its end 5 mm, and this desilvered section is coated with a silicone lacquer chosen for high surface resistivity; (*b*) 20 cm^3/min of dry air is pumped over the bender during operation; (*c*) the insulated end section of the bender is interrupted by a grounded section made by wrapping a 200-μm grounded gold wire around it; (*d*) the brass strip (Fig. 1 C) which separates the two oppositely polarized ceramic layers of the bender is grounded by this same wire.

There is no avoiding a boundary between the probe and the air-water interface. Experience with early probe models showed that movement of this boundary often introduced large artifacts. Presumably these artifacts arose from the movement of charges which are known to be concentrated at such a boundary and to be responsible for so-called electrocapillary effects. This boundary was immobilized and these electrocapillary artifacts were avoided by the 'inner boundary setter' shown as part 6 in Fig. 1. This component is made from a no. 1 glass cover slip. Its edge is hand sharpened with abrasive paper and its upper surface waxed with solid paraffin. Meniscus movement was further reduced by the use of culture chambers with side walls about as high above the specimen plane as the inner boundary setter (Fig. 1 A). Thus the meniscus could be kept nearly flat. In practice we find it advantageous to use enough fluid to give a meniscus curved a few tenths of a millimeter *below* its boundaries, but this is not very critical.

The vibrating probe and specimen are usually viewed under bright-field illumination with a Zeiss UPL inverted microscope. The vibrating probe is thus perceived as two pale but sharp images at the two limits of its vibration. (Fig. 2 is a photograph of the higher-contrast images shown by stroboscopic illumination.) The vibrating probe is translated with an XYZ micropositioner controlled by three micrometers with 2.5-μm divisions (Line Tool Co., Allentown, Pa., model H-2). The microscope and micropositioner are clamped to a 190 kg machinist's surface plate mounted upon rubber isolators to yield a system with a natural frequency of 9 Hz. The instrument is used in a room thermostated to keep the air temperature near the microscope within a 1°C range.

Fabrication

Micropipettes of maximum taper are made on a one-stage vertical puller by drawing them at the lowest temperature which does not give shattered tips. They are vacuum plated with a just opaque layer of gold in a zone between 0.6 mm of the tip and a few millimeters of the other end. A gold-plated brass sleeve is cemented to each pipette with epoxy cement toward its drawn end and with silver-filled conductive epoxy toward its other end. The silver-filled epoxy is sealed off by applying thermosetting silicone rubber to the sleeve's top end. These "shells" are now stored indefinitely until needed.

Each shell is then converted to a platinum-black tipped probe through an appropriate variation of the well-known "indium" technique (11). It is held vertical on the mechanical stage of a horizontally placed microscope with a clamp whose lower face is thermally insulated. Its tip is broken off to a 5 μm diameter by gently lowering it against a glass surface which is slightly tilted so as to show the lowered tip approaching its own reflection. A 2.4-mm long piece of wire made from Cerrotru[1] solder is dropped into the shell. "Anchored sockets" are prepared by soldering the eye end of a Singer no. 9 sewing needle (Singer Co., New York), into a cut-down no. 24 Twistcon microminiature socket (from Microdot Inc., South Pasadena, Calif.) with 60:40 Sn-Pb solder. Such a socket is held by friction on a tool consisting of a Teflon-coated needle with a handle. It is thus inserted into the shell. The shell is centered in a single nichrome loop with its tip 0.5 mm below the loop. The loop is heated to melt the solder while one presses gently down on the tool until it reaches the desired level. (To avoid forming gaps in the solder, it should be melted in 30 s or less.) Then the heating and pressure are stopped. Upon cooling, the socket is well attached to the Cerrotru solder (the needle's eye prevents the otherwise frequent delayed disconnection of the socket and solder), and a bead of solder 0.2–0.3 mm in diameter protrudes from the tip. Sometimes the bead is connected directly to the tip but often it is connected by a narrow neck region which may be anywhere from 10 μm to centimeters in length. We tend to get higher quality probes if a neck has been present at this stage.

The solder is put at -1.50 V with reference to a gold plating solution (0.2% AuKCN), and the bead knocked off by rapidly lowering the shell's tip into the solution and then suddenly stopping this motion. Thus gold plating starts immediately at the freshly broken solder face. The voltage is then adjusted to give an initial current of 5 nA and gold is deposited until a 9-μm wide bead is formed. This takes about 10 min.

The tip is then rinsed in two changes of distilled water and dipped into a platinizing solution (1% chloroplatinic acid + 0.01% lead acetate) without any immediate application of voltage. The subsequent application of voltage is guided by our discovery that with any fixed voltage, over a range from 0.5 to 1.2 V or more, platinization follows a curious two-stage course. During the first stage, lasting 20–80 s, a relatively spongy layer forms. It is seen to grow relatively quickly in thickness, appears remarkably black by reflected light, and forms an interface with a relatively low impedance but insufficient adherence to the gold. In the second stage, metal seems to be laid down in part within the interstices of the first deposit to make it more compact. This second stage is indicated by a sudden shift to a lower rate of thickening with little change in current and the deposition of much grayer, more reflective material. It forms an interface with higher impedance but much greater mechanical stability.

We combine sufficient adherence with minimal impedance by forming undercoats via two-stage deposition followed by an overcoat stopped during the first stage. Typically, we first adjust the voltage to 0.6–0.8 V so as initially to deliver 0.2 μA and we maintain this voltage for 2 min (and thus go through both stages) to form a first, 2-μm thick undercoat. Then we raise the voltage by 0.2 V and maintain this second voltage for another 2 min, and thus again go through both stages to form a second, 1-μm thick undercoat. Finally, we increase the voltage by yet another 0.2 V and maintain this third voltage until we produce a 5-μm thick, spongy overcoat and a total electrode diameter of about 25 μm.

We then platinize the outer, reference electrode at 0.3 mA for 7 min, rinse the probe with distilled water, dip it into seawater, and check its noise output at 200 Hz. At present it takes 1–2 h to convert a shell into a complete and tested probe, and about one half of these prove satisfactory.

A probe cannot be put into the vibrator freehand. It is held with a tool consisting of a rod attached to a no. 24 Twistcon pin. The rod slides in a guide tube which can be swiveled into a position coaxial with the probe holder sleeve, and the probe is then slipped in. Before insertion, the lower end of the holder sleeve is lightly greased with high-vacuum silicone grease chosen for its high viscosity so as to prevent upward creep of the seawater during use.

A good probe can usually be used for several weeks before it becomes too noisy and must be replatinized or replaced. Replatinizing is often effective in restoring low noise, particularly when some reduction in probe diameter, evidently due to platinum loss, has occurred. It is most conveniently done with the probe still in the vibrator.

RESULTS

Mechanical

The vibrating probe is made to measure current, but its electrical performance depends upon its

[1] Cerro Corp., New York. This is an alloy of 58% bismuth and 42% tin which melts at 138°C, wets glass, and expands by 5 μm/cm while solidifying.

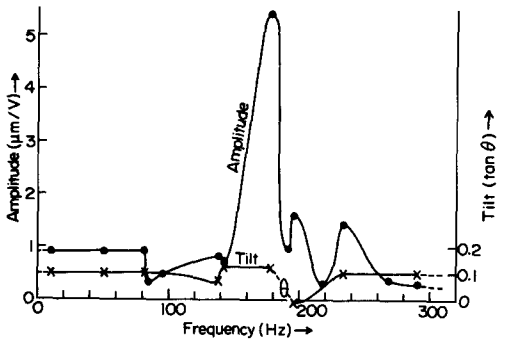

FIGURE 4 Vibration direction and amplitude of a typical vibrating probe. Tilt indicates the observed angle between the ball's vibration direction and the normal to the probe's axis. This axis in turn was supposed to be parallel to that of the bender's plane, but could have been tilted by as much as 10° off that plane. The ellipse at about 190 Hz is meant to suggest the elliptical vibration observed near that frequency. Amplitude indicates the peak-to-peak vibration amplitude of the ball per peak to peak voltage applied to the bender.

mechanical behavior. So we will first report some observations upon the latter.

The system is expected to vibrate the test electrode in a single horizontal direction normal to the bender. To check this, we have made numerous observations with both steady and stroboscopic illumination. They have never shown any detectable vertical component of the vibration. Fig. 4 summarizes a study of a typical probe's movement within the horizontal plane. Over almost the whole range of frequencies studied, from 10 to 300 Hz, the vibration was indeed linear (and about normal to the reed). However, in a narrow range from about 188 to 194 Hz, it was noticeably elliptical; at 191 Hz, where this was most pronounced, the vibration ellipse had a long axis of 23 μm normal to the reed and 4 μm along it. We never use the probe at a frequency yielding detectable ellipticity.

Fig. 4 also shows the amplitude of vibration per volt applied to the bender. The main features of this curve are those expected of a cantilevered vibrating reed with a relatively large mass at its free end. There is a sharp main resonance at a frequency close to that estimated from measurements of the probe's mass and the bender's compliance. There are also two secondary resonances which we do not fully understand.

We routinely work with a vibration amplitude of about 30 μm. We know of no difficulty in vibrating at lower amplitudes. A maximum amplitude, on the other hand, may be set by the tendency for arcing to occur between the bender's faces above 40 V; this would set a 100–200 μm amplitude limit in our present system.

The above studies were done in seawater. In order to test the effect upon the probe's vibration of raising the medium's viscosity, we added various concentrations of a commercial viscogen to the seawater (Dow Chemical's 15,000 centipoise 90 HG methocel, Dow Chemical U.S.A., Midland, Mich.). According to the manufacturer's reports, 1.2% and 2.0% concentrations of this viscogen should have raised the viscosity by 1,000- and 10,000-fold, respectively, yet we found these concentrations to reduce the probe's vibration amplitude (per bender voltage at resonance) by only 10% and 40%, respectively. Evidently, the vibration amplitudes of probes immersed in low-viscosity aqueous media like seawater are not at all limited by external drag.

While the medium exerts little drag on the probe, the probe greatly stirs the medium. We observed this stirring by suspending some 0.8-μm polystyrene latex spheres in the medium. We focused our attention on the region near the vibrating ball. Using a 30-μm ball vibrating one ball diameter, we saw the expected small (1–10 μm) oscillations of the suspended particles; but we also saw an unexpected unidirectional flow pattern. The gross features of this pattern seen in the vibration plane are sketched in Fig. 5. The vibrating probe is seen to pump fluid steadily out of its ball end, and to form two main vortices which are *not* symmetrical. (It is interesting that an essentially similar pattern has been predicted for, and to a limited degree observed within the region nearest to a simple sphere oscillating with a relatively small amplitude [12]). Superimposed upon the oscillatory flow and the steady, unidirectional flow is a turbulent zone extending out about a ball diameter in front of the vibrating ball.

At a few hundred Hz in seawater, steady flow rates near a ball vibrating 30 μm are about 30–3,000 μm/s. These rates fall as the viscosity, η, is raised. We observed the steady velocity at one position near the ball and found it to vary with $\eta^{-0.8}$ as η was raised from 40 to 12,000 centipoise via Methocel addition. These rates likewise fall as the amplitude, L, is reduced. In a medium of 40 centipoise viscosity, we observed the steady velocity at another point near the ball to vary with $L^{2.5}$ as it was lowered from 30 μm to 5 μm. (The theory

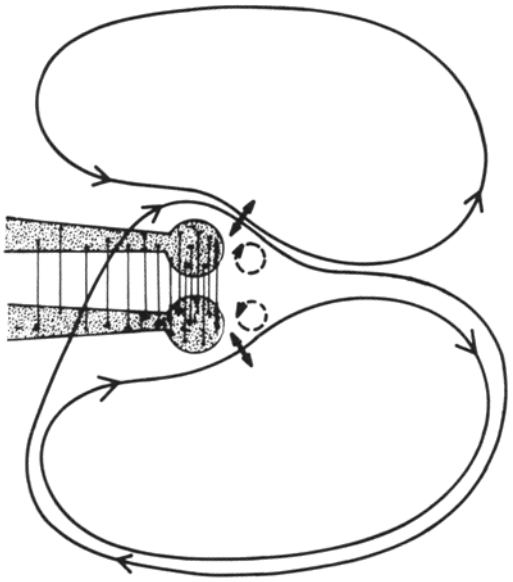

FIGURE 5 Gross features of the flow pattern produced by a vibrating probe. This flow has three main components: (*a*) two large-scale, steady, unidirectional vortices indicated by the solid lines. Note the typical asymmetry shown by the (relatively slow) flow across the probe's shaft; (*b*) a turbulent region indicated by the dashed circles; (*c*) superimposed oscillatory flow at the vibration frequency. The double-headed arrows indicate its direction and magnitude where this oscillatory component is largest. Sketched from visual observations of 0.8-μm marker particles near a 30-μm diameter probe vibrating at 210 Hz.

of a simple sphere oscillating with a relatively small amplitude predicts L's exponent to be about two [12]).

Responses to Known Currents

We will report the probe's electrical performance largely in terms of current densities rather than potential gradients for two reasons: first, because a cell's membrane generally offers a far higher resistance to current flow than does the extracellular medium, hence current densities should be relatively independent of the medium's resistivity, while voltage gradients should be proportional to it; second, because the current densities normal to the inside and the outside of any element of the plasma membrane are equal (13), while intracellular voltage gradients can be inferred from extracellular measurements only with the aid of additional information including the identities of the ions which carry the current across the membrane as well as the mobilities of these ions within the cell.

A lock-in amplifier works by inverting every other half-cycle of the input signal so as to give a DC output. The phase control knob on the instrument allows one to determine the phase of the inversion point in this key operation. When we drive a steady current through the region of test electrode vibration, the output shows the expected sinusoidal variation with this phase, so we always begin to use the probe by setting the phase to maximize the output.

We generally use a resonant frequency since a minimal bender voltage should minimize the danger of arcing across the bender. However, frequencies within a few Hertz of harmonics of 60 Hz, e.g. 181 Hz, must be avoided due to power-line interference.

We find the vibrating probe system to respond to known current densities in the theoretically expected way over a very wide range of conditions. The system's output voltage should indicate a peak-to-peak voltage input given by:

$$V = \cos\theta\ (L\rho\delta), \tag{1}$$

where θ is the angle between current and vibration directions in this region, L is the peak-to-peak amplitude of the probe's vibration, ρ is the resistivity of the medium, δ is the current density in the region probed.

The actual responses to known current densities were tested by driving a known current, I, through the medium. This current was generated by a Keithley model 261 picoammeter source (Keithley Instruments, Inc., Cleveland, Ohio), and was led into the medium via two Ag-AgCl electrodes and seawater-filled micropipettes. The pipettes' tips were 6 mm apart and the vibrating ball was placed within a few hundred micrometers of one of them. Here the current should have spread radially to give a current density given by:

$$\delta = I/4\pi r^2, \tag{2}$$

where r is the distance to the closer tip.

A typical recording of such a measurement, with the vibration in the current's direction, is shown in Fig. 6 (left). This measurement is within experimental error of equation (1). In Fig. 6 (right) we plot the result of a series of similar recordings in which θ was varied from $+90°$ to $-90°$. Again, the results are within experimental error of the values

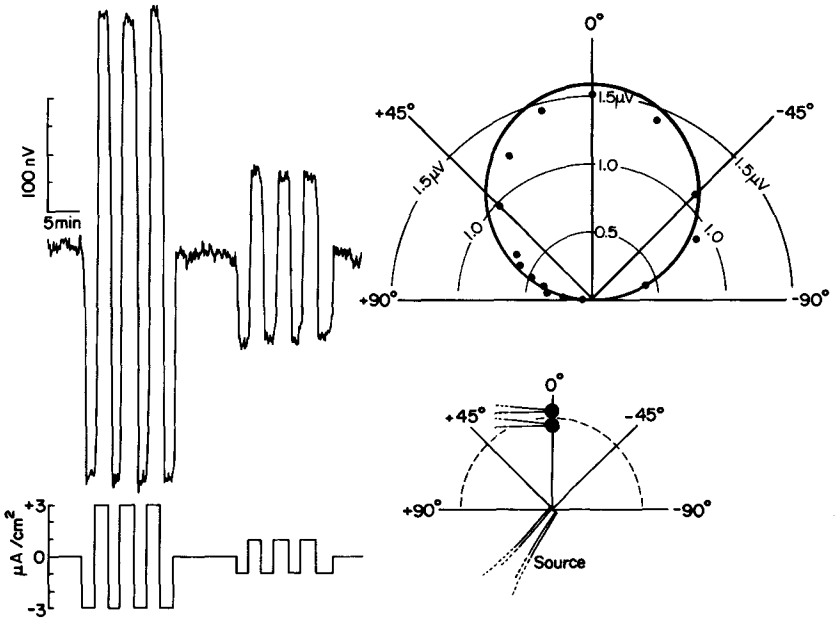

FIGURE 6 Responses of a vibrating probe to known currents. The medium was seawater with a resistivity of 24 Ω-cm, the vibration amplitude was 30 μm, and the time constant, 10 s. Left, The vibration was in the direction of the local current. The course of current densities shown below yielded the voltage output shown above. Right, The angle, θ, between the vibration and current directions was varied. This was done by keeping the vibration direction fixed and moving the probe over a semicircular path as shown below. The resulting voltage values are shown in the polar plot above. The circle represents the voltages predicted by equation (1).

given by equation (1). With currents parallel to the vibration, equation (1) has likewise been verified (to within ±10%) over a range of resistivities of 24–10,000 Ω-cm, a range of amplitudes of 3–60 μm, and a range of current densities from 0.02 to 200 μA/cm².

Barrier Artifacts

To obtain a reliable base line for steady current measurements, we first shift the vibrating ball horizontally to a reference position which is far from the object whose field is to be explored; then we move the vibrating ball into the object's field for measurements. For example, to measure the field about a 50-μm radius fucoid embryo, we first shift the ball to a reference position 200–300 μm away. Since a current dipole's field falls off with the inverse cube of the distance from its center (14), the egg's field should be negligible there.

However, we have encountered a recurrent and insidious "barrier artifact" when a vibrating probe is then returned to a position near any barrier to current flow, even an egg-sized glass bead. The system then registers a voltage change which seems to indicate a current originating in the bead; but of course, it has quite another origin. In our experience, such signals are usually produced by a current leaking from the bender into the medium (and hence to ground via the probe). In the absence of a barrier, such a leakage current flows at about 90° to the vibration direction and thus is not registered at all, or is registered as a small, steady signal indistinguishable from other sources of base-line shift when the bender is energized. A barrier, however, diverts such a current so as to raise its component in the vibration direction. Measurements of such a barrier artifact are shown in Fig. 7 A. We have also encountered barrier artifacts with the different pattern about a glass bead shown in Fig. 7 B. This latter proved to originate in a current generated by a corrosion battery in the connector to the probe (part 2, Fig. 1).[2]

[2] Barrier artifacts are practically eliminated when the platinum black reference electrode (pt. 19, Fig. 1) is shifted to the under side of the inner boundary setter (pt. 6, Fig. 1).

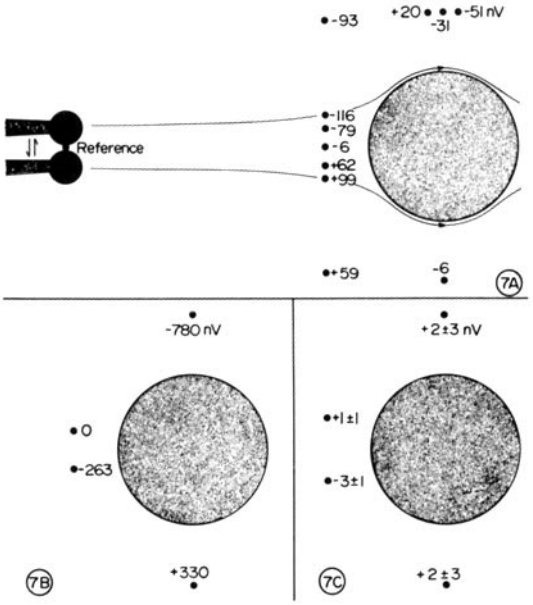

FIGURE 7 Detection of barrier artifacts with a glass bead. Each value is a nanovolt difference determined along a 30-μm step centered about the indicated point and in the vibration direction shown in 7 A; moreover, each is with respect to a reference measurement as shown in 7 A. Positive and negative values indicate current components flowing towards and away from the bottom of the page, respectively. 1 nV indicates a current density of 14 nA/cm^2 in the seawater medium used. The test bead was 120 μm in diameter and the vibration frequency about 200 Hz. In the experiment summarized in 7 A, we inferred that the artifacts arose from the diversion around the bead of current leaking into the medium from the bender. Two such current lines are illustrated (15). In 7 B, the artifacts were mainly produced by current driven into the medium by a corrosion battery in the connector to the signal cable. In 7 C, careful insulation, shielding, and avoidance of corrosion have practically eliminated barrier artifacts.

Finally, the reader may wonder if these barrier artifacts, when they do occur, may not originate in *streaming potentials* rather than leakage current distortion. We rejected streaming potentials as an explanation because we found the carrier artifact to be unaffected upon introducing 1% protamine sulfate into the medium and thus presumably reversing the sign of all the surface charges in the system; to be unaffected upon raising the medium's viscosity 10,000-fold with Methocel and thus radically reducing both steady and turbulent flow rates; and to depend only upon the square of the vibration amplitude rather than the higher power expected for a streaming potential mechanism.

Interference by Polyelectrolyte Gradients

A cell whose field is being explored might well release polyelectrolytes, such as proteins or sulfated polysaccharides, which ionize into relatively sluggish macromolecules with mobile counter ions. Outward diffusion of such substances so as to reach a higher concentration at one end of the ball's vibration path than the other might in turn give a measurable potential. We will call such a potential a Donnan potential though it might with equal justice be called a liquid junction potential; the two are equivalent in this case. The probe's mixing action would be expected to reduce the signals so produced, but the reliable calculation of this attenuation seems impractical. So we explored this question experimentally.

To do this, we fabricated artificial sources of polyelectrolyte gradients which were designed to give relatively large diffusion gradients of roughly known size, to have a shape and size similar to those of some cell protrusions, but to generate no current. We formed 1.3-mm OD glass tubing into 11-mm long micropipettes with 30-μm diameter tips. The wide end of each pipette was sealed with an elastic cap made of heat-shrinkable Teflon tubing plugged with Teflon rod. The tubing was then pinched and released so as to fill the end 2–3 mm of a pipette with a warm aqueous solution of a polyelectrolyte, 3% NaCl and 2% agar. Such a source was affixed to the bottom of a specimen chamber with grease and covered with a 3% NaCl solution. 10–70 min later we measured the voltage gradient just in front of it. (To be exact, the gap between the pipette's open tip and the closest position was set at about 10 μm.) We tested five polyelectrolytes, all of which have about 200–300 daltons per charge and which span a range of mol wt from 440 to about 2×10^7. The measured voltage differences as well as the results of certain calculations needed for their interpretation are shown in Table 1.

One of these latter is an estimate of the polyelectrolyte concentration at the source's tip at the time of measurement. We obtain this through the analysis of the following theoretical model: we suppose that the region just outside the source's tip is always approximated by the steady state which exists outside of a spherical source. The

TABLE I

Response of Vibrating Probe to Polyelectrolyte Gradients in 25 Ω-cm Saline

Substance	mol wt (daltons)	D	Tip concentration		ΔV(nV)*		Largest ratio
			Start	While measuring‡	Measured	Expected without probe‡	
		cm^2/s	%	%	nV	nV	
A. Resonant frequency (200–244 Hz) 30-μm amplitude							
Dextran sulfate	2×10^7	7×10^{-8}	1	0.06	−28, +17, +34, +17, −14	+11,000	0.003
			0.1	0.008	+3, −2 (NS)	+1,600	
	3×10^5	4×10^{-7}	1	0.02	−143, +63, +13, +88, +1, +12	+4,200	0.03
			0.1	0.004	+7, −7 (NS)	+740	
Heparin	10^4	1.4×10^{-6}	1	0.02	+7, +4 (NS)	+4,400	
Protamine	5×10^3	2×10^{-6}	1	0.02	+10, +2	−3,400	0.003
Tri-glu§	440	4×10^{-6}	1	0.01	+9, +1 (NS)	+2,000	
			0.1	0.001	−1 (NS)	+200	
B. 7 Hz, 15-μm amplitude							
Dextran sulfate	2×10^7	7×10^{-8}	1	0.11	−984, −2, 0	+11,000	0.09
			0.1	0.007	−6 (NS)	+700	
	3×10^5	4×10^{-7}	1	0.03	+3,000; +9,000; +230	+3,000	3
			0.1	0.003	+390, +25	+300	1.3
Tri-glu§	440	4×10^{-6}	0.1	0.0008	+33	+84	0.4

Each voltage difference represents the change observed or expected when the probe is moved from a reference position to one 10–20 μm from a 30-μm source pipette containing the indicated substance.

* Positive values indicate a rise in potential in moving away from the source. NS means not significantly different from zero.

‡ From equations (6–8) for the source immersal times corresponding to the largest ΔVs measured.

§ Glutamyl-glutamyl-glutamate.

concentration, C_s, at the surface of such a source is given by

$$C_s = -a(\mathrm{d}C/\mathrm{d}r)_s, \tag{3}$$

where a is the sphere's radius, and r is the distance from the sphere's center.

We further suppose that the region within the pipette is in the nonsteady state produced in a semi-infinite pipe which starts at the time $t = 0$ with a uniform concentration C_0 and then loses material through diffusion from its open end in a manner governed by the boundary condition (3) and the diffusion constant D. The solution of this model is formally equivalent to that given by Carslaw and Jaeger (16) for the surface temperature of a semi-infinite slab at a constant initial temperature and radiating heat at a rate proportional to the surface temperature. When appropriate conversions from heat diffusion to material diffusion are made, one obtains:

$$C_s/C_o = e^{x^2} \cdot erfc(x), \tag{4}$$

where

$$x = (Dt)^{1/2}/a, \tag{4 a}$$

and a is the pipe's radius.

In our experiments, x was > 3. For such large x values:

$$e^{x^2} \cdot erfc(x) \cong 1/\pi^{1/2}x. \tag{5}$$

Hence

$$C_s = C_o \cdot a(\pi Dt)^{-1/2}, \tag{6}$$

which is the desired solution.

It also helps interpretation to estimate the potential difference which should exist between the two points compared by the vibrating probe in the absence of stirring or other disturbance by the probe itself. In the steady state, the difference in polyelectrolyte concentration, ΔC, between two points outside of a spherical source is given by:

$$\Delta C = aC_s \cdot \Delta(1/r), \tag{7}$$

which for a 30-μm vibration amplitude and the other dimensions used is about 0.2 C_s.

If C_s is that of a 1% solution of a polyelectrolyte bearing one charge per 200 daltons, it involves a charge concentration of 0.05 mol/liter. Hence the pertinent difference in relatively immobile charges is 0.01 M. From Davies and Rideal (17), one obtains the Donnan potential, Ψ, produced by a relatively low concentration of immobilized charges, P, in a sodium chloride concentration, S, as:

$$\Psi = RT\,P/2S, \tag{8}$$

where R is the gas constant and T is the absolute temperature.

For P equal to 0.01 M and for 3% NaCl, this is about 200,000 nV. So this is the voltage difference expected per 30 μm in the absence of the probe when C_s is 1%. When C_s falls to a lower value, the undisturbed potential difference should be proportionally lower.

With these two calculations available, we can now consider Table I. The most important observation is that when the estimated source concentration falls below 0.01%, a probe vibrating at the resonant frequency yields no significant signal. However, with an estimated 0.02% source solution of the 3×10^5 mol wt polyanion, with a 0.06% source solution of the 2×10^7 mol wt polyanion, and possibly the 0.02% solution of the 5×10^3 mol wt polycation, significant signals are registered by a probe at resonance. These signals are highly variable, and for 4 of the 11 significant values they are actually in the direction opposite to that expected in the absence of the probe. However, it remains clear that the probe's vibration greatly attenuates such effects at resonance. The *largest* values recorded are only 0.003, 0.03, and 0.003 times the values expected in the probe's absence for 2×10^7, 3×10^5, and 10^4 mol wt polyelectrolytes, respectively.

One may roughly summarize these data as an indication that vibration at resonance generally discriminates against Donnan potentials (as opposed to current-generated potentials) by about 100–1,000-fold. Vibration at the relatively low frequency of 7 Hz, however, is far less effective in discriminating against Donnan potentials. Only 3 of the 10 measured values indicate a discrimination factor better than 10-fold.

Other Artifacts

It proves possible to replace the medium in the course of 1–2 min without producing a detectable artifact, provided only that its conductivity is kept constant. To avoid disturbance, we add new medium and remove old medium at equal rates, and also place the inlet and outlet well below the medium's surface. Influx and efflux are equalized by using two equal-bore 10 cm^3 glass syringes with rigidly linked plungers, so that as fluid is expelled from one, an equal amount is pulled into the other.

Relatively large and slow changes in the ambient air temperature can change the output by up to 2 nV/1°C; in practice we avoid such artifacts by keeping the ambient air within a 1°C range with a control system that cycles in 1–10 min. Thermally mediated artifacts can also be produced by heating up the specimen with the microscope's illumination light, but this is easily avoided by using heat filters.

Finally, we may note that the vibrating probe system is relatively immune to external electrical interference. Thus, while the operation of a stroboscope produces huge artifacts, and switching a light on or off may give quite a blip, other common sources of interference such as the continuous operation of nearby pump or fan motors, or of fluorescent lights have given no trouble.

Noise

Fig. 8 shows the root mean square current density noise, δ_n, generated by a typical 25-μm diameter vibrating probe in media of various resistivities, ρ, and at various vibration frequencies. In each case a time constant of 10 s was used. In each case, also, δ_n was obtained by dividing the rms voltage noise by ρL. The rms voltage noise, in turn, was taken to be 0.25 of the average peak-to-peak voltage noise measured over periods of 100 s which is 10 time constants. The various media were obtained by adding NaCl to distilled water. Their resistivities ranged from that of seawater (~25 Ω-cm), to that of vertebrate blood serum (~100 Ω-cm), to that of most pondwaters (1,600–6,400 Ω-cm). We will therefore refer to the 100 Ω-cm medium as "serum" and the 6,400 Ω-cm medium as "dilute pondwater."

In each case, δ_n is compared with the theoretical minimum attainable current density noise, $\bar{\delta}$, generated by the access resistance to the probe. When

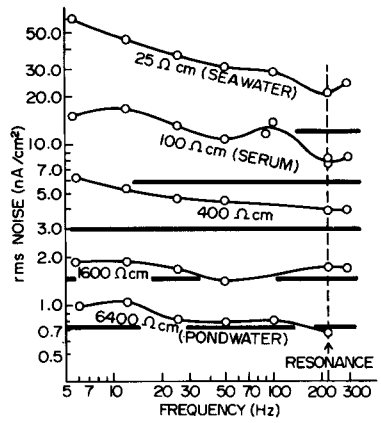

FIGURE 8 Current density noise of a typical vibrating probe as a function of medium resistivity and vibration frequency. For each medium, the probe's noise, -O-O-, is compared with the theoretical minimum noise (or Johnson noise), generated by the access resistance. The minimum noise limit lines are truncated for the two lowest resistivity media to avoid overlap. The lock-in amplifier's time constant was set at 10 s; the bender's resonant frequency was 220 Hz; the test electrode's diameter was 25 μm and its vibration amplitude set at 30 μm; the temperature was 15°C.

account is taken of the test electrode's stem, this access resistance, $\bar{R}$, is given approximately by:

$$\bar{R} \cong \rho/10a, \tag{9}$$

where a is the test electrode's radius
moreover

$$\bar{\delta}_n = \rho^{-1}(kT\bar{R}/\tau)^{1/2} \tag{10}$$

where k is Boltzmann's constant, T is the absolute temperature, τ is the lock-in's time constant.
Hence:

$$\bar{\delta}_n = (kT/10a\rho\tau)^{1/2}. \tag{11}$$

δ_n is seen to be smallest at the main resonant frequency of 220 Hz, and it shows the expected steady decline with increasing ρ. Thus at resonance, it goes from 20 nA/cm² in seawater to 0.7 nA/cm² in dilute pondwater.

Furthermore, δ_n is seen to approach $\bar{\delta}_n$ more and more closely as ρ rises. Thus, in seawater at resonance, δ_n is only 70% higher than the theoretical minimum, $\bar{\delta}_n$, in serum, 30% higher, while in dilute pondwater there is no longer *any* significant difference.

Finally, in order to analyze the residual excess noise, i.e. $(\delta_n - \bar{\delta}_n)$, we also measured the noise produced by substituting wire-wound resistors having the calculated access resistance, $\bar{R}$ for the vibrating probe. These simulated access resistance noise values usually proved to be closer to δ_n than to $\bar{\delta}_n$. It follows that most of the residual extra noise is generated by the amplifying system rather than by the vibrating probe. Examination of the manufacturer's specifications supports this inference and indicates that most of the extra noise arises from an impedance mismatch between the probe and the preamplifier. So, at least at resonance, it should be possible to remove most of the residual excess noise either by adding an impedance matching transformer to the system or by appropriately replacing the preamplifier.

The above data were determined with the lock-in's time constant set at about 10 s. If τ is varied, the noise should be proportional to $\tau^{-1/2}$. We have verified this expectation over the range from 30 s down to about 0.3 s, using a probe vibrating at a resonant frequency with a 30-μm amplitude in sea water.

Application

Figs. 2 and 9 illustrate our first application of the vibrating probe. If one places it in front of the growing tip of a two-celled fucoid embryo (as photographed in Fig. 2 and diagrammed in Fig. 9 *a*), one observes characteristic pulses of current *entering* its growing tip (18). On the other hand, if one vibrates the probe normal to any part of such an embryo which is far from the growing tip (e.g. the rhizoid cell's base as shown in Fig. 9 *b*), then one observes similar, though weaker pulses *leaving* the embryo. Systematic study allows one to plot a self-consistent current dipole field during such pulses. Such endogenous current pulses have not been previously observed to transverse fucoid embryos, and presumably, could not have been detected before development of the vibrating probe. However, it may be noted that they are consistent with previous electrical measurement using the series method (8), as well as with recent measurements of tracer influx asymmetry (1), in indicating an endogenous current loop through the developing fucoid embryo which enters the growing tip and leaves elsewhere.

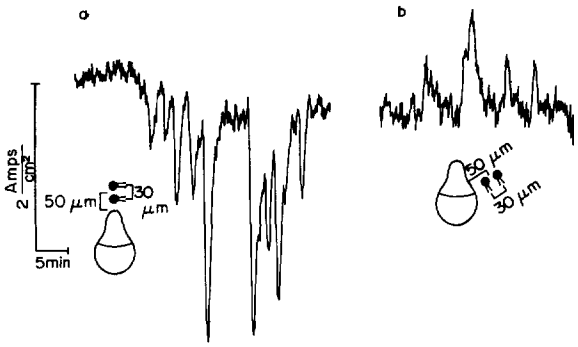

FIGURE 9 Current pulses generated by a growing, 1-day old *Pelvetia* embryo measured with a 25-μm diameter probe vibrating at 200 Hz in the diagrammed positions. Seawater medium. Temp = 15°C. Downward movement of the tracing indicates current entering the embryo.

DISCUSSION

Resolving Power

Using a vibrating probe system with a time constant, τ, of 10 s and a 30-μm diameter platinum-black test electrode vibrating with an amplitude of 30 μm to measure fields in seawater, we find a voltage resolution of 1–2 nV and an inferred current density resolution of about 20 nA/cm². There is a trade-off between temporal resolution which is set by τ, spatial resolution which is jointly determined by the test electrode's diameter and vibration amplitude, and current density resolution which is mainly set by the probe's resistance. Increases in temporal resolution attained by reducing τ must be traded for decreases in current density resolution since current noise depends upon $\tau^{-½}$. If the vibration amplitude is much larger than the test electrode's diameter, this amplitude sets the spatial resolution in the vibration direction, and any effort to increase spatial resolution by reducing the amplitude must obviously be traded for a proportionate reduction in current density resolution. Finally, if this amplitude is much smaller than the test electrode, then the latter's diameter sets the spatial resolution, and improvements in spatial resolution attained by reducing this diameter must be traded for some reduction in current density resolution since smaller electrodes have larger resistances and hence larger noise, though how much larger remains to be explored.

Comparison with Other Methods

In an earlier, unpublished investigation we made an intensive effort to attain the utmost in voltage (and inferred current) resolution using a pair of conventional, static, seawater-filled micropipettes to measure extracellular fields. Suffice it to say that with the same, roughly 30-μm spatial resolution and the same, roughly 10-s temporal resolution, the best voltage (and current) resolutions so attained were no better than 100 nV (and a few μA/cm²), thus about 100 times poorer than those now attained with the vibrating probe system. The only similar measurements of steady extracellular currents that we know of are those of Hagins et al. (7), who used static saline-filled micropipette pairs to determine such currents outside of rat retinal rod cells. While these measurements were not closely comparable to ours, they clearly suggest a comparable, 100-nV limit.

Finally, one may ask just why medium-filled micropipettes prove to be two orders of magnitude less sensitive than a comparable vibrating probe. Calculations indicate that one order of magnitude is accounted for by the small solid angle subtended by a micropipette's orifice internally as compared to that subtended externally, and thus to the high resistance of a micropipette's interior as compared to the access resistance. The origin of the other 10-fold discrepancy is less clear; though it seems to be mainly attributable to some combination of local, composition-dependent "tip potentials", true electrode (as contrasted with pipette or salt bridge) noise, and DC amplifier noise.

Limitations and Extensions

The vibrating probe now registers only one component of the current in a small region at a time. We anticipate development of a "stereo probe", one made to vibrate in two (or even three?) orthogonal directions simultaneously, which would thus allow the simultaneous measurement of two

(or perhaps even three) components of the current in a region. A two-dimensional stereo probe might be vibrated by reverse use of the sort of piezoelectric mechanism used in stereophonic records, while it could be readily monitored with a so-called two-phase lock-in amplifier accessory.

We anticipate the development of probes with smaller balls at their tips. These should allow for greater spatial resolution at the possible expense of reduced current sensitivity.

We also anticipate improvements in accuracy through the study of distortions in the current field produced by the probe. With the uniform test currents employed so far, probe distortion has no effect on the output because the current field is necessarily distorted to an equal degree at every point of the probe's vibration. That is why equation (1) is found to be truly independent of the vibration amplitude. With nonuniform fields, however, errors may well be introduced by probe distortion. At relatively low frequencies, the ball's surface impedance will be so high as to force current to diverge around it; whereas at relatively high frequencies, the ball's impedance will be lower than that of the medium, and current should converge to cross it. It follows that at some intermediate frequency, where the ball's impedance approximates that of the medium, such distortion should be minimal. In short, frequency-controlled impedance mtaching could serve to minimize errors introduced by probe distortion in nonuniform fields.

Exploratory experiments indicate that a probe vibrating at resonance discriminates against voltage gradients produced by polyelectrolyte diffusion (as opposed to those generated by electrical currents) by the order of 100–1,000-fold. Our judgement is that this should prove sufficient protection against polyelectrolyte interference in all but the most unusual cases. Thus, suppose that a living cell actually released some material similar to the 3×10^5 mol wt dextran sulfate which gave the greatest interference of all of the polyelectrolytes tested. This cell would have to maintain a concentration of 0.01% of this material at its surface in order to give measurable interference in seawater. Yet simple diffusion calculations show that if a 100-μm diameter cell released this stuff at a steady, uniform rate great enough to maintain its surface concentration at 0.01%, then it would be using up about 10% of its total dry weight per hour. That should not happen very often.

Finally, we anticipate that, unlike fucoid eggs, some cells will be seriously disturbed by a vibrating probe nearby. How could one obtain the needed mechanical protection without interrupting electrical currents from the cell being studied? We find that one way is to grow the cells on one side of a thin, ion-permeable membrane[3] and vibrate the ball near its other side. Significant accessory advantages of such a membrane method should be greater protection against polyelectrolyte interference as well as against barrier artifacts.

We are glad to acknowledge M. V. L. Bennett's essential help in bringing Davies' rather obscure abstract to our attention, as well as Dr. Davies' subsequent willingness to discuss unpublished details with us. We would also like to thank Messrs. E. Henss and T. Van Rijk of our machine shop for their skilled fabrication of the tiny parts needed.

This investigation was financially supported by a National Science Foundation research grant to L. F. Jaffe and a National Institutes of Health biophysics training grant to Richard Nuccitelli. The central idea developed was in P. W. Davies' 1966 abstract (9).

Received for publication 15 April 1974.

REFERENCES

1. JAFFE, L. F., K. R. ROBINSON, and R. NUCCITELLI. 1974. Local cation entry and self-electrophoresis as an intracellular localization mechanism. *Ann. N. Y. Acad. Sci.* In press.
2. KINOSITA, H. 1963. Electrophoretic theory of pigment migration within fish melanophores. *Ann. N. Y. Acad. Sci.* **100**:992.
3. WOODRUFF, R. I., and W. H. TELFER. 1973. Polarized intercellular bridges in ovarian follicles of the *Cecropia* moth. *J. Cell Biol.* **58**:172.
4. LUND, E. J. 1947. Bioelectric fields and growth. University of Texas Press, Austin, Tex.
5. TASAKI, I., and N. KAMIYA. 1964. A study on electrophysiological properties of carniverous amoebae. *J. Cell. Comp. Physiol.* **63**:365.
6. NOVÁK, B., and F. W. BENTRUP. 1972. An electrophysiological study of regeneration in *Acetabularia mediterranea*. *Planta (Berl.)*. **108**:227.
7. HAGINS, W. A., R. D. PENN, and S. YOSHIKAMI. 1970. Dark current and photocurrent in retinal rods. *Biophys. J.* **10**:380.
8. JAFFE, L. F. 1966. Electrical currents through the

[3] For example, ultrathin (about 1 μm) regenerated cellulose membranes made by North Star Research Institute, Minneapolis.

developing *Fucus* egg. *Proc. Natl. Acad. Sci. U. S. A.* **56:** 1102.

9. DAVIES, P. W. 1966. Membrane potential and resistance of perfused skeletal muscle fibers with control of membrane current. *Fed. Proc.* **25**:332.
10. GESTELAND, R. C., B. HOWLAND, J. Y. LETTVIN, and W. H. PITTS. 1959. Comments on microelectrodes. Proc. IRE **47**:1856.
11. FRANK, K., and M. C. BECKER. 1964. *In* Physical techniques in biological research. W. L. Nastuk, editor. Academic Press Inc., New York. 33.
12. BOOTH, T. C. 1973. Higher-order effects associated with steady streaming about a vibrating sphere. Ph.D. Dissertation, Purdue University, Lafayette, Indiana. 99, 145.
13. PLONSEY, R., and D. G. FLEMING. 1969. Bioelectric phenomena. McGraw-Hill, Inc., New York. 217.
14. JAFFE, L. F., K. R. ROBINSON, and B. F. PICOLOGLOU. 1974. A uniform current model of the endogenous current in an egg. *J. Theor. Biol.* **45**:593.
15. COLE, K. C. 1968. Membranes, ions, and impulses. University of California Press, Berkeley, Calif. 17.
16. CARSLAW, H. S., and J. C. JAEGER. 1959. Conduction of heat in solids. 2nd. ed. Clarendon Press, Oxford, England, 70, 483.
17. DAVIES, J. T., and E. K. RIDEAL. 1963. Interfacial phenomena. 2nd ed. Academic Press Inc., New York. 82.
18. NUCCITELLI, R., and L. F. JAFFE. 1975. Spontaneous current pulses through developing fucoid eggs. *Proc. Natl. Acad. Sci. U.S.A.* In press.